# 无 机 化 学 学 报

2017 年　　第 33 卷　　第 8 期


## 目　次

### 综　述


碳硼烷硼氢键选择性官能团化的研究进展……李欢欢　燕　红　芦昌盛(1313)


### 论　文


金属有机框架材料对[Fe(HB(pz)$_3$)$_2$]自旋转换行为的影响(英文)
……赵　田　Ishtvan Boldo　Christoph Janiak　刘跃军(1330)
激光诱导游离色氨酸对血红蛋白反应动力学影响及机理
……曹洪玉　史　飞　唐　乾　郑学仿(1339)
$Bi_{4-x}Eu_xTi_{3-y}M_yO_{12}$(M=Fe,Co,Ni)纳米颗粒的制备及光学和磁学性能
……葛　文　杨培志　申兰先　邓书康(1349)
面向异丁烷脱氢介孔 $\gamma$-$Al_2O_3$ 基催化剂的合成及其高催化性能
……刘越洋　郑小琴　杨建华　Waseem Raza　鲁金明　殷德宏　张　艳(1357)
可循环 SERS 基底 ZnO/Ag 纳米材料合成和表征(英文)……黄庆利　李　靖　魏文娴(1365)
1,10-菲咯啉 Cu(Ⅱ)配合物修饰碳糊电极的电催化析氢性能……刘利娟　王　燕　何建波(1374)
由 4-甲基-1,2,3-噻二唑-5-甲酸构筑的过渡金属配合物的合成、晶体结构及与 DNA 作用
……严世承　胡未极　沈金杯　赵国良(1381)
金@氧缺陷二氧化钛核壳纳米颗粒的制备及光催化产氢
……寇书芳　封振宇　王春省　杨　剑(1390)
双(3,5-二叔丁基水杨醛)缩卡巴肼二丁基锡配合物的微波溶剂热合成、结构及除草活性
……杨春林　冯泳兰　张复兴　庾江喜　蒋伍玖　邝代治　阳年发(1397)
阴阳离子聚氨酯/羟基磷灰石复合微球的制备及其自组装
……赖　欣　侯　毅　李玉宝　黄　敏　任　欣　张　利(1403)
CoSAPO-34 分子筛的合成、表征及其光催化脱氮性能……罗五魁　陈　峰　颜桂炀　白云山(1411)
脱合金制备纳米多孔双金属氧化物 $NiMoO_4$ 及其电化学性能
……周　琦　郑　斌　李志洋　王亚飞　冯基伟(1416)
高振实密度圆饼状 $LiFePO_4$/C 的制备及电化学性能……吴仪娜　周　乐　徐国庆　黄　洁
方　雄　王　涛　刘文明　晋　媛　汪　洋　唐新村(1423)
4-氯-2-(1*H*-咪唑并[4,5-*f*][1,10]菲咯啉)苯酚铜(Ⅱ)配合物的晶体结构及其与 DNA 的相互作用
……寇莹莹　任相浩(1429)
介孔调变对 CuY 催化剂甲醇氧化羰基化反应活性的影响
……阎立飞　张国强　李艳娇　郑华艳　李　忠(1435)
基于[1,2,4]-三唑衍生物的两个镉(Ⅱ)配合物的结构与光谱学表征
……王大伟　王　滔　闫　桐　杜　琳　赵琦华(1443)

高压实富镍正极材料 $LiNi_{0.85}Co_{0.06}Mn_{0.06}Al_{0.03}O_2$ 的制备
……胡国荣　谭潮溥　杜　柯　彭忠东　曹雁冰　梁龙伟　王伟刚(1450)
退火温度对 $TiO_2$/CdSe 纳米片异质结薄膜光电性能的影响
……朱留东　武军伟　薛晋波　钱　凯　胡兰青(1457)
4-(2-(4-咪唑)苯乙烯基)吡啶和三种芳香二羧酸的 Cd(Ⅱ)配位聚合物的合成、结构及荧光性质
……梁　蕊　王玉停　郭永康　轩小朋(1465)
一个富路易斯碱位配合物的合成、结构及对痕量 $Ag^+$的荧光检测(英文)
……辛凌云　李云平　鞠丰阳　李晓玲　刘广臻(1474)
肟型 Schiff 碱 Cu(Ⅱ)和 Ni(Ⅱ)配合物的合成、晶体结构及光谱性质(英文)
……郭建强　孙银霞　俞　彬　李　璟　贾浩然(1481)
1,2-环己二胺缩邻香兰素单核与四核镱稀土配合物的近红外性质(英文)
……范仲天　高　博　董艳萍　邹晓艳　李光明(1489)
苯基或联苯基桥连双环戊二烯基铼羰基化合物的合成、结构及催化性能(英文)
……张　宁　马志宏　李素贞　韩占刚　郑学忠　林　进(1497)

# CHINESE JOURNAL OF INORGANIC CHEMISTRY

**Vol.33 No.8 Aug. 2017**


## CONTENTS

### Cover



Effect of Metal-Organic Frameworks on the Spin-Transition Behavior of $[Fe(HB(pz)_3)_2]$ (English)

ZHAO Tian, Ishtvan Boldog, Christoph Janiak, LIU Yue-Jun

DOI:10.11862/CJIC.2017.178

*Chinese J. Inorg. Chem.*, **2017**,**33**:1330-1338


### Reviews


Progress in Selective B-H Bond Functionalization of Carborane

LI Huan-Huan, YAN Hong, LU Chang-Sheng

DOI:10.11862/CJIC.2017.166

*Chinese J. Inorg. Chem.*, **2017**,**33**:1313-1329


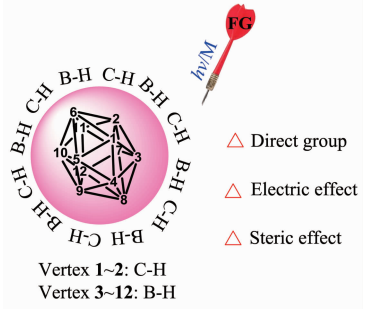


The specific-site selective functionalization of carborane, that can be controlled by direct group, electric or steric effect, is very highly desirable. Now, the related examples about cage B-H bond functionalization were outlined in detail.

### Articles


Effect of Metal-Organic Frameworks on the Spin-Transition Behavior of $[Fe(HB(pz)_3)_2]$ (English)

ZHAO Tian, Ishtvan Boldog, Christoph Janiak, LIU Yue-Jun

DOI:10.11862/CJIC.2017.178

*Chinese J. Inorg. Chem.*, **2017**,**33**:1330-1338


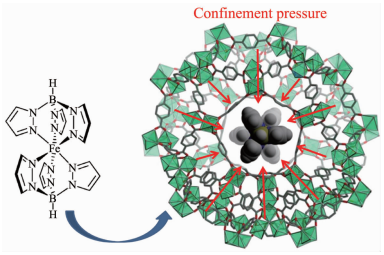


The well investigated spin-crossover compound $[Fe(HB(pz)_3)_2]$ was embedded in the pores of two mesostructured metal-organic frameworks MIL-101(Cr) and MIL-100(Al) to yield SCO@MOF composites. Compared to bulk phase $[Fe(HB(pz)_3)_2]$, the embedded $[Fe(HB(pz)_3)_2]$ molecules are isolated by the pores of MOFs, which present different spin transition behavior.

## Effect and Mechanism of Laser-Induced Hemoglobin Reaction Kinetics with Free Tryptophan

CAO Hong-Yu, SHI Fei, TANG Qian, ZHENG Xue-Fang

DOI:10.11862/CJIC.2017.159
*Chinese J. Inorg. Chem.*, **2017**,**33**:1339-1348

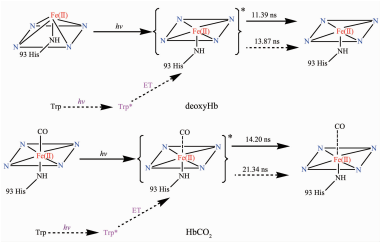


According to transient absorption, kinetics curve and UV-Vis absorption spectra, the iron-porphyrin of four forms of hemoglobin could be excited by incident light or by the energy transfer from excited state tryptophan, and then decayed to the state of plane porphyrin structure and six-coordinated Fe with one ligand vacancy.

## Synthesis, Luminescent and Magnetic Performance of $Bi_{4-x}Eu_xTi_{3-y}M_yO_{12}$ (M= Fe/C/Ni) Nanoparticles

GE Wen, YANG Pei-Zhi, SHEN Lan-Xian, DENG Shu-Kang

DOI:10.11862/CJIC.2017.180
*Chinese J. Inorg. Chem.*, **2017**,**33**:1349-1356

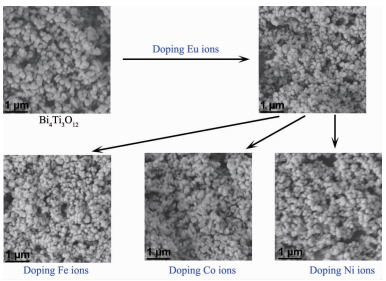


By doping luminescent and magnetic ions, the $Bi_{4-x}Eu_xTi_{3-y}M_yO_{12}$ nanoparticles present smaller particle sizes and uniform morphologies. The luminescent intensity is strongest when the Eu ions concentration reached to 0.4. Moreover, the luminescent intensity increased gradually by decreasing the magnetic ions concentration. Besides, the products have good ferromagnetic properties.

## Synthesis and Catalytic Performance of Mesoporous $\gamma$-$Al_2O_3$ Catalyst for Isobutane Dehydrogenation

LIU Yue-Yang, ZHENG Xiao-Qin, YANG Jian-Hua, Waseem Raza, LU Jin-Ming, YIN De-Hong, ZHANG Yan

DOI:10.11862/CJIC.2017.138
*Chinese J. Inorg. Chem.*, **2017**,**33**:1357-1364

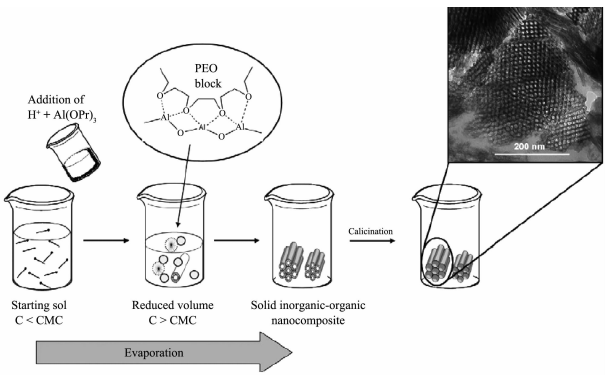


## Synthesis and Characterization of ZnO/Ag Nanocomposites for Recyclable Surface-Enhanced Raman Scattering Substrate (English)

HUANG Qing-Li, LI Jing, WEI Wen-Xian

DOI:10.11862/CJIC.2017.168
*Chinese J. Inorg. Chem.*, **2017**,**33**:1365-1373

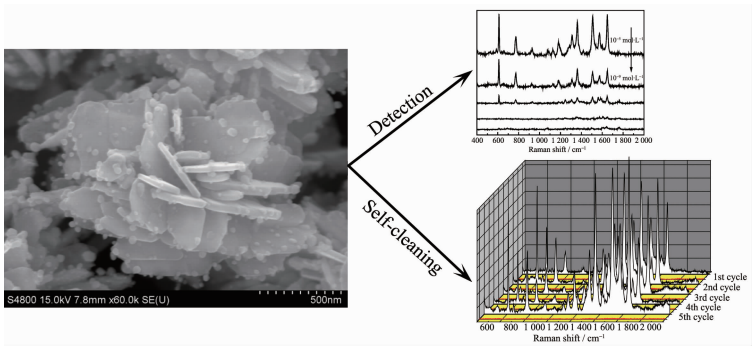


ZnO/Ag flower-like nanocomposites as self-cleaning surface enhanced Raman scattering substrates were obtained by a simple one-step hydrothermal method.

## Cu(Ⅱ) Complex Based on 1,10-Phenanthroline as an Efficient Electrocatalyst for Hydrogen Evolution Reaction

LIU Li-Juan, WANG Yan, HE Jian-Bo

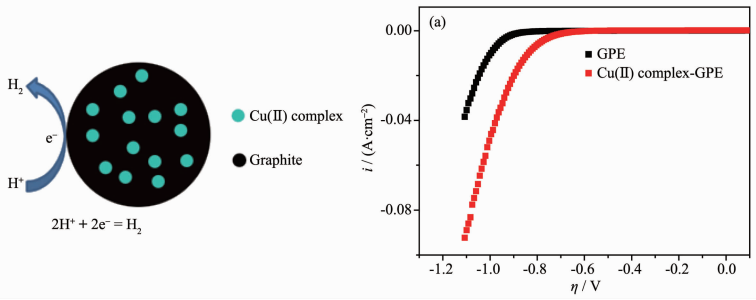


Cu (Ⅱ) complex based on 1,10-phenanthroline and 5-sulfaisophthalate was firstly mixed with graphite paste to form a work electrode for the hydrogen evolution reaction in acid media, exhibiting improved HER performace than bare GPE.

DOI:10.11862/CJIC.2017.131
*Chinese J. Inorg. Chem.*, **2017**,**33**:1374-1380

## Syntheses, Crystal Structures and DNA Binding of Transition Metal Complexes Constructed by 4-Methyl-1,2,3-thiadiazol-5-carboxylic Acid

YAN Shi-Cheng, HU Wei-Ji, SHEN Jin-Bei, ZHAO Guo-Liang

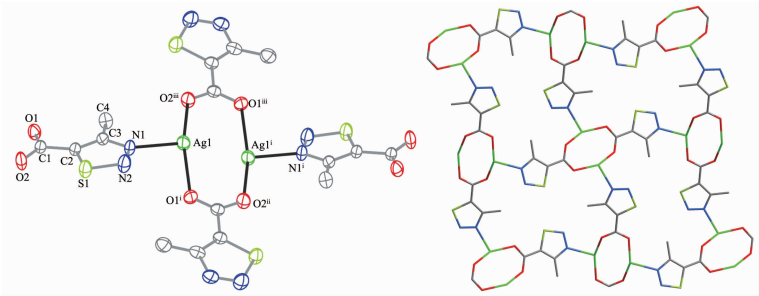


Complex $[AgL]_n$ (HL =4-methyl-1,2,3-thiadiazol-5-carboxylic acid) crystallizes in monoclinic system with space group $P2_1/c$, and it forms a deformation plane triangle configuration with 2D network structure.

DOI:10.11862/CJIC.2017.177
*Chinese J. Inorg. Chem.*, **2017**,**33**:1381-1389

## Facile Synthesis of Core-Shell Au@H-$TiO_2$ Nanoparticles for Photocatalytic Hydrogen-Generation

KOU Shu-Fang, FENG Zhen-Yu, WANG Chun-Sheng, YANG Jian

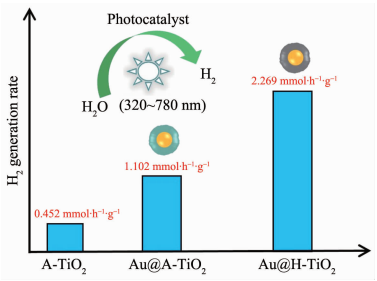


$H_2$ production rate of core @shell Au@H-$TiO_2$ can be improved to 2.269 mmol·$h^{-1}$·$g^{-1}$ compared with that of A-$TiO_2$ (0.452 mmol·$h^{-1}$·$g^{-1}$). The enhancement may be attributed to the synergistic effect of oxygen vacancies, $Ti^{3+}$ species and Au core, which significantly promote charge transfer and inhibit charge recombination.

DOI:10.11862/CJIC.2017.161
*Chinese J. Inorg. Chem.*, **2017**,**33**:1390-1396

## Microwave-Solvent Thermal Syntheses, Crystal Strutures and Herbicidal Activity of Bis(3,5-Di-*t*-Butylsalicylaldehyde) Carbohydrazide Dibutyltin Complexes

YANG Chun-Lin, FENG Yong-Lan, ZHANG Fu-Xing, YU Jiang-Xi, JIANG Wu-Jiu, KUANG Dai-Zhi, YANG Nian-Fa

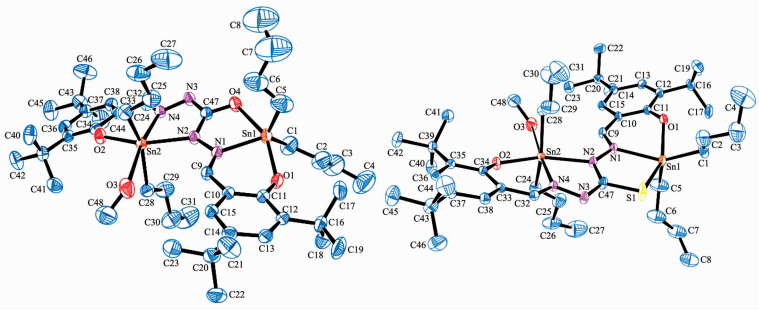

The dibutyltin (Ⅳ) binuclear complexes exhibit herbicidal activity for *Portulaca oleracea*, *Amaranthus spinosus* and *Semen cassiae*.

DOI:10.11862/CJIC.2017.175
*Chinese J. Inorg. Chem.*, **2017**,**33**:1397-1402

## Preparation and Self-Assembly of Oppositely Charged Polyurethane/ Hydroxypatite Microspheres

LAI Xin, HOU Yi, LI Yu-Bao, HUANG Min, REN Xin, ZHANG Li

DOI:10.11862/CJIC.2017.164
*Chinese J. Inorg. Chem.*, **2017**,**33**:1403-1410

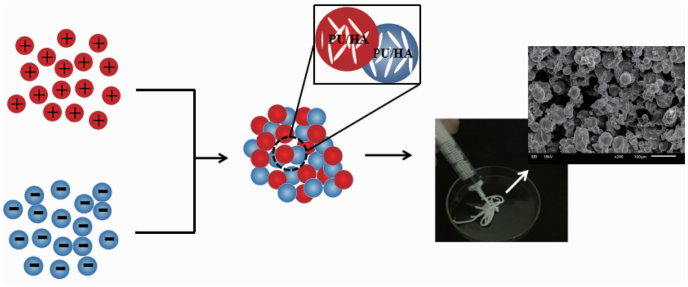


## Synthesis, Characterization and Photocatalysis Denitrification Properties of CoSAPO-34 Molecular Sieve

LUO Wu-Kui, CHEN Feng, YAN Gui-Yang, BAI Yun-Shan

DOI:10.11862/CJIC.2017.160
*Chinese J. Inorg. Chem.*, **2017**,**33**:1411-1415

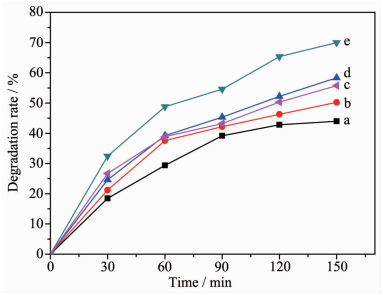


The CoSAPO-34 molecular sieves showed good crystallinity and still remained structure of SAPO-34 with good thermal stability, and the photocatalytic degradation ratio reached to 70% under the irradiation of 500 W Xe lamp for 150 min.

## Preparation and Electrochemical Performance of Nanoporous $NiMoO_4$ by De-alloying

ZHOU Qi, ZHENG Bin, LI Zhi-Yang, WANG Ya-Fei, FENG Ji-Wei

DOI:10.11862/CJIC.2017.145
*Chinese J. Inorg. Chem.*, **2017**,**33**:1416-1422

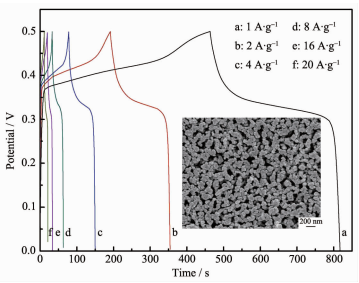


The nano-porous $NiMoO_4$ obtained by de-alloying and annealing shows excellent supercapacitor performance due to the pinning effect of the Mo element on the de-alloying reduction of the skeleton and pore size of the porous alloy. Its current density is 708 $F \cdot g^{-1}$ at 1 $A \cdot g^{-1}$, and when the current density increases by 20 $A \cdot g^{-1}$, the specific capacity retention rate of 57.1%.

## Synthesis and Electrochemical Properties of Cake-like $LiFePO_4$/C with High Tap Density

WU Yi-Na, ZHOU Le, XU Guo-Qing, HUANG Jie, FANG Xiong, WANG Tao, LIU Wen-Ming, JIN Yuan, WANG Yang, TANG Xin-Cun

DOI:10.11862/CJIC.2017.163
*Chinese J. Inorg. Chem.*, **2017**,**33**:1423-1428

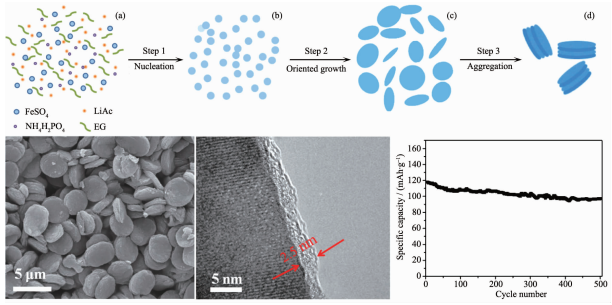


## Crystal Structure and DNA Interaction Property of Cu(Ⅱ) Complex with 4-Chloro-2-(1*H*-imidazo[4,5-*f*][1,10] phenanthrolin-2-yl)phenol

KOU Ying-Ying, REN Xiang-Hao

DOI:10.11862/CJIC.2017.157
*Chinese J. Inorg. Chem.*, **2017**,**33**:1429-1434

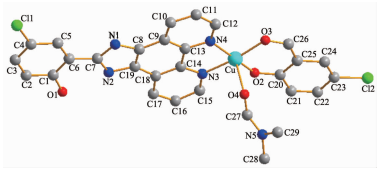

The complex $[Cu(L)(5\text{-}Cl\text{-}sal)(DMF)]ClO_4 \cdot DMF$ can interact with CT-DNA and cleave circular pBR322 plasmid DNA with addition of hydrogen peroxide which mechanism is likely to involve singlet oxygen $^1O_2$ and hydroxyl radical ·OH as reactive oxygen species.

## Influence of Mesoporous Modulation on CuY Catalyst for Oxidative Carbonylation of Methanol

YAN Li-Fei, ZHANG Guo-Qiang, LI Yan-Jiao, ZHENG Hua-Yan, LI Zhong

DOI:10.11862/CJIC.2017.172
*Chinese J. Inorg. Chem.*, **2017**,**33**:1435-1442

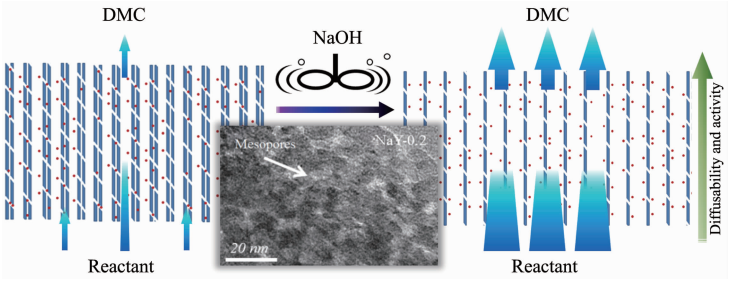


## Crystal Structures and Spectroscopic Characterizations of Two Cd(Ⅱ) Complexes Based on [1,2,4]-triazole Derivatives

WANG Da-Wei, WANG Tao, YAN Tong, DU Lin, ZHAO Qi-Hua

DOI:10.11862/CJIC.2017.185
*Chinese J. Inorg. Chem.*, **2017**,**33**:1443-1449

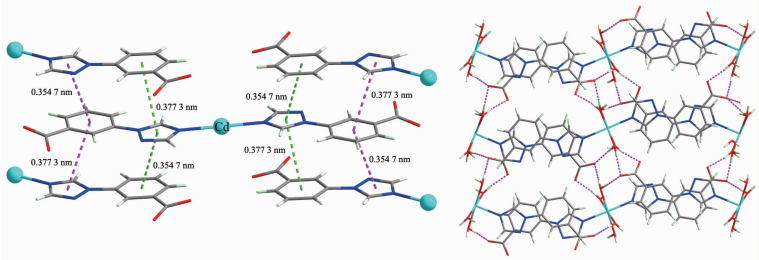


## Synthesis of Ni-Rich Layered $LiNi_{0.85}Co_{0.06}Mn_{0.06}Al_{0.03}O_2$ Cathode Material with High Compacted Density

HU Guo-Rong, TAN Chao-Pu, DU Ke, PENG Zhong-Dong, CAO Yan-Bing, LIANG Long-Wei, WANG Wei-Gang

DOI:10.11862/CJIC.2017.169
*Chinese J. Inorg. Chem.*, **2017**,**33**:1450-1456

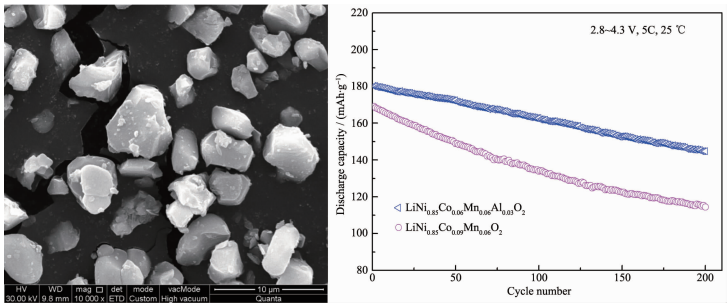


## Effect of Annealing Temperature on Photoelectric Characteristics of $TiO_2$/CdSe Nanosheet Heterojunction Thin Films

ZHU Liu-Dong, WU Jun-Wei, XUE Jin-Bo, QIAN Kai, HU Lan-Qing

DOI:10.11862/CJIC.2017.183
*Chinese J. Inorg. Chem.*, **2017**,**33**:1457-1464

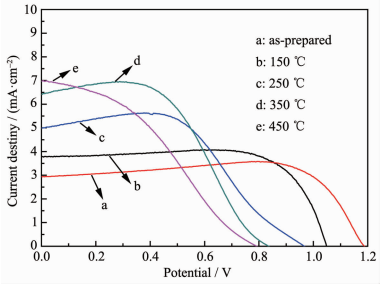


With the increase of the annealing temperature, the photocurrent density of the $TiO_2$/CdSe nanosheet heterojunction thin films increases, but the open circuit voltage and the filling factor decreases, which leads to a reduction in the efficiency of photoelectric conversion.

## Syntheses, Structures and Fluorescent Properties of Cadmium Coordination Polymers with 4-(2-(4-Imidazole)styryl) pyridine and Three Aromatic Dicarboxylic Acids

LIANG Rui, WANG Yu-Ting, GUO Yong-Kang, XUAN Xiao-Peng

DOI:10.11862/CJIC.2017.154
*Chinese J. Inorg. Chem.*, **2017**,**33**:1465-1473

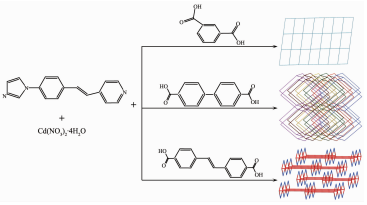

Three new coordination polymers based on $Cd(NO_3)_2 \cdot 4H_2O$, ISPE and dicarboxylic acids were synthesized by the solvothermal reaction. Due to the difference of dicarboxylic acids, diversity crystal structures were obtained. The fluorescence properties of the three cadmium complexes were investigated.

## Synthesis, Structure and Luminescent Detection for Trace $Ag^+$ of a Coordination Polymer with Lewis Basic Sites (English)

XIN Ling-Yun, LI Yun-Ping, JU Feng-Yang, LI Xiao-Ling, LIU Guang-Zhen

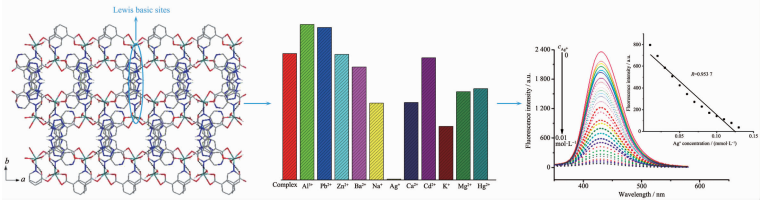


A supramolecular network containing Lewis basic N sites may not only accomplish an effective and reliable quantitative testing method for pure $Ag^+$ ion with a detection range of $10^{-4}$~$10^{-6}$ mol·$L^{-1}$ concentration limit, but also display selective sensing of $Ag^+$ ion in colorless solution.

DOI:10.11862/CJIC.2017.184
*Chinese J. Inorg. Chem.*, **2017**,**33**:1474-1480

## Syntheses, Crystal Structures and Spectroscopic Properties of Copper(Ⅱ) and Nickel(Ⅱ) Complexes with Oxime-Type Schiff Base Ligands (English)

GUO Jian-Qiang, SUN Yin-Xia, YU Bin, LI Jing, JIA Hao-Ran

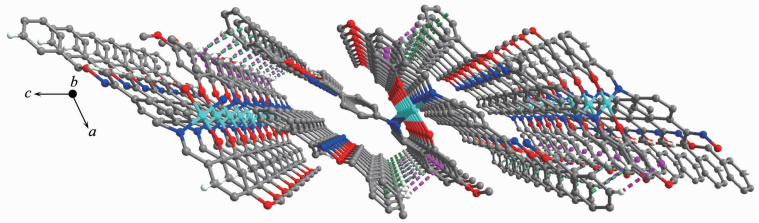


Two oxime-type Schiff base mononuclear Cu(Ⅱ) and Ni(Ⅱ) complexes form a 3D and 2D supramolecular structures via different intermolecular interactions (C–H···$\pi$ and $\pi$···$\pi$ stacking interactions, respectively).

DOI:10.11862/CJIC.2017.181
*Chinese J. Inorg. Chem.*, **2017**,**33**:1481-1488

## NIR Luminescent *N*,*N*′-Bis(3-methoxy-salicylidene)cyclohexane-1,2-diamine Mono- and Tetra-nuclear Ytterbium Complexes (English)

FAN Zhong-Tian, GAO Bo, DONG Yan-Ping, ZOU Xiao-Yan, LI Guang-Ming

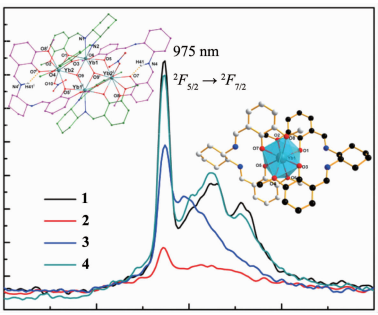


Four salen type ytterbium complexes featuring an ionic crossover mononuclear and a defect-dicubane structure have been isolated. All complexes exhibit the similar typical NIR luminescence of $Yb^{3+}$ ions proposing that the energy transfer from ligands to $Yb^{3+}$ ions takes place effectively.

DOI:10.11862/CJIC.2017.182
*Chinese J. Inorg. Chem.*, **2017**,**33**:1489-1496

## Syntheses, Structures and Catalytic Activity of *p*-Phenylene- or *p*-Biphenylene-Bridged Biscyclopentadienyl Dinuclear Rhenium Carbonyl Complexes(English)

ZHANG Ning, MA Zhi-Hong, LI Su-Zhen, HAN Zhan-Gang, ZHENG Xue-Zhong, LIN Jin

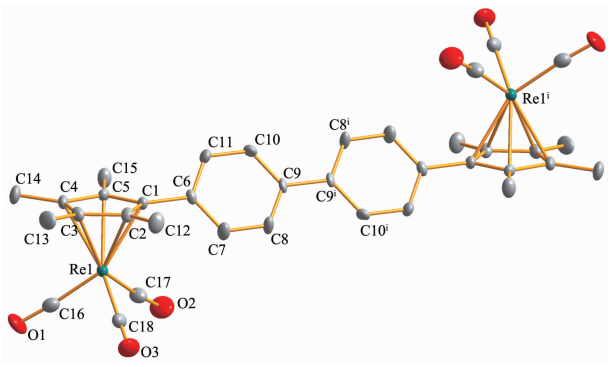


DOI:10.11862/CJIC.2017.153
*Chinese J. Inorg. Chem.*, **2017**,**33**:1497-1504